THE ASTROPHYSICAL JOURNAL, 470:629–635, 1996 October 10

A LONG-DURATION SOLAR FLARE WITH MASS EJECTION AND GLOBAL CONSEQUENCES

H. S. HUDSON[1]
Institute for Astronomy, University of Hawaii, Honolulu, HI 96822

L. W. ACTON
Montana State University

AND

S. L. FREELAND
Lockheed Palo Alto Research Laboratory

Received 1995 October 19; accepted 1996 April 16

ABSTRACT

We report observations of a long-duration flare with mass ejection from the corona, using the *Yohkoh* soft X-ray telescope (SXT). This flare occurred 1994 November 13 near disk center during quiet solar conditions, with excellent temporal coverage of both the core activity in the active region itself and of the global corona. The initial X-ray images reveal two arcades of cusped magnetic loops, connected via a series of thin loops. These loops rise rapidly during the increasing phase of soft X-ray flare brightness. In its final state, the flare has the configuration of postflare loops with a cusp. Large regions of the X-ray corona appear to empty during the evolution of the event. We suggest that this corresponds a coronal mass ejection (CME) seen in soft X-rays. Its detection in the SXT images is consistent with the finding that material participating in a CME exists at elevated coronal temperatures (2.8×10^6 K in this case) before the ejection. We estimate a mass $>4 \times 10^{14}$ g for the ejected material. The X-ray morphology of the event has strong points of similarity with the classical reconnection picture of long-duration event (LDE) formation, but there are significant discrepancies: there is no observed inward flow during the rise phase, the expansions are multiple and appear to be nonradial, and none of the observed motions suggest a reconnection jet. We note the subsequent occurrence of very large scale coronal disturbances, including regions near the boundaries of coronal holes at both poles. We suggest that this global disturbance implies a perturbation reaching as far outward as the heliospheric neutral sheet. The exciter would require a horizontal velocity of approximately 200 km s^{-1} in such a case, consistent with the projected velocity of the plasma cloud that we identify with a CME in the process of launching.

Subject headings: Sun: corona — Sun: flares — Sun: magnetic fields — Sun: particle emission

1. INTRODUCTION

The *Yohkoh* soft X-ray telescope (SXT) enables us to see the entire X-ray corona with good time resolution. With this capability, we can follow the evolution of a flare event in detail and learn a great deal about its geometry. We employ SXT observations to address the important problem of the linkage between the development of an eruptive flare (or other disturbance in the lower corona) and the formation of a coronal mass ejection (CME). There is no consensus yet on the physical nature of the flare/CME link. Certainly, full confidence in any theoretical description will require detailed knowledge of the geometry, and it is for this reason that the *Yohkoh*-SXT observations will play an important role.

In this paper, we report a recent event in which SXT systematically observed both large and small scales during just the right phases of the development of a classical long-duration event (LDE), the type of flare event associated most closely with coronal mass ejections. Because this event reached only the C2 level, the *Yohkoh* flare mode did not trigger. Accordingly, we have uninterrupted sequences of full-Sun images as well as the usual high-resolution images of the core of the event. Perhaps because this event developed at a time of extremely quiet conditions, the faint large-scale phenomena could be observed more clearly than in similar events occurring during times of greater activity. This paper describes this event in some detail, with reference to an earlier LDE flare from the same active center. Previous *Yohkoh* observations of events of related types have been described by McAllister et al. (1992), Tsuneta et al. (1992a, 1992b), Hiei, Hundhausen, & Sime (1993), Hanaoka et al. (1994), Khan et al. (1994) and Watanabe et al. (1994).

This paper depends mainly upon careful consideration of the SXT image morphology. This may be a tedious matter for most readers, especially because they do not have access to the movie representations of the data that make many of the dynamical effects so much easier to see. Accordingly, we have put much of the descriptive text in the Appendix, and we proceed directly here with what we believe that we can see and reliably infer. The "roadmap" Figures 1 and 2 (Plate 7) show the general layout of the events discussed. A reader uninterested in the details could, in fact, even skip the following section and proceed directly to the conclusions (§ 3).

2. ANALYSIS

2.1. *Outward Flows*

During the rise phase, this event exhibits expansion to the north from its core regions. The composite image in Figure 3 (Plate 8) shows the relationship between the core of the

[1] Institute of Space and Astronautical Science, Japan.

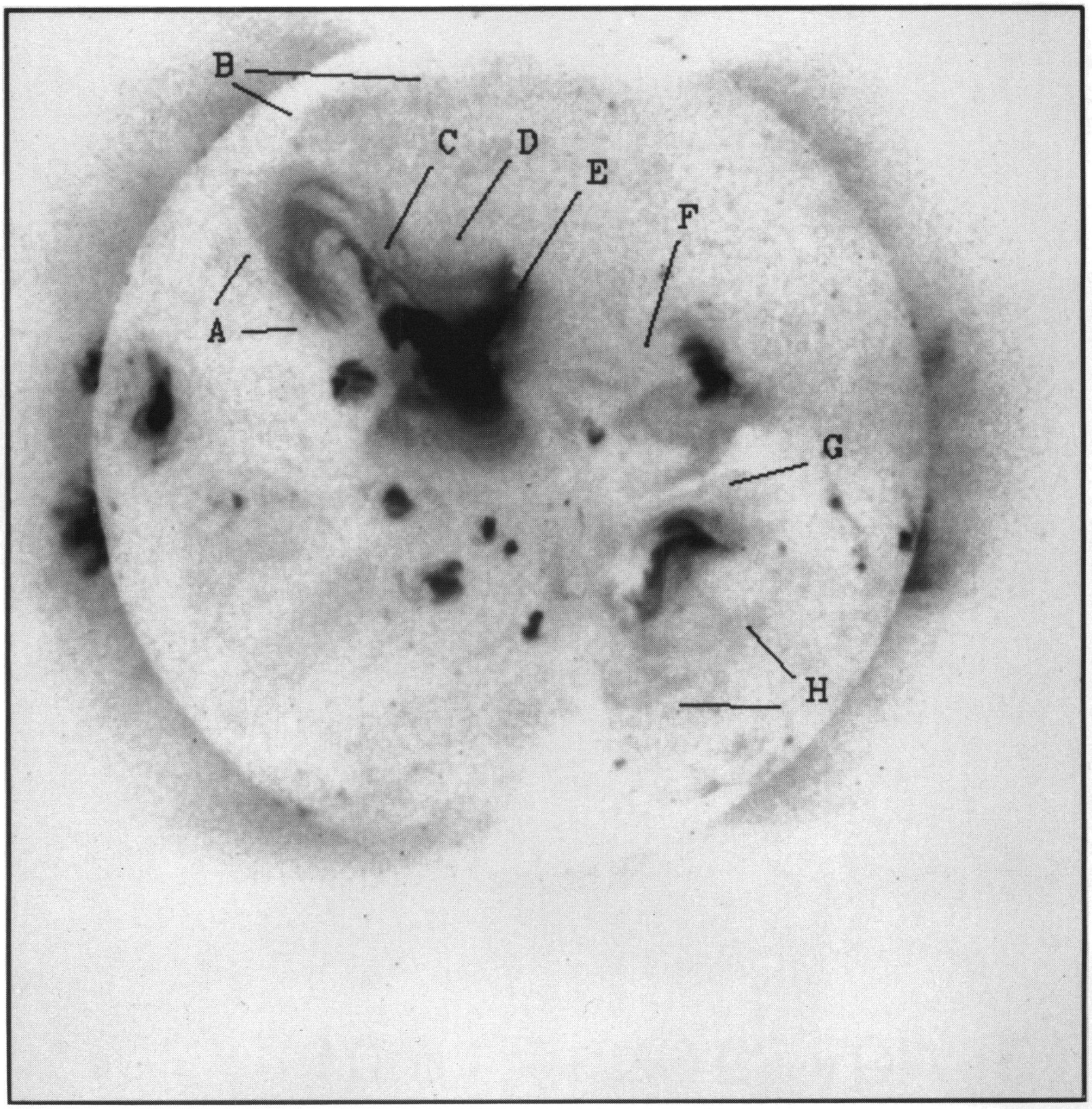

FIG. 2.—Image road map to the event studied here: composite image from the SXT "Dagwood" (AlMg) filter taken 1994 November 13 at 11:29:35 UT, with labels indicating the locations of features discussed in the text: (*a*) the "disappearing cloud" whose mass is estimated as 4×10^{14} g; (*b*) northern polar region of diffuse brightening; (*c*) the northeast cusped ejection; (*d*) the region of east-west "links"; (*e*) the northwest cusped ejection; (*f*) region of interconnecting loops; (*g*) another region of interconnecting loops; (*h*) southern polar region of diffuse brightening and ejection.

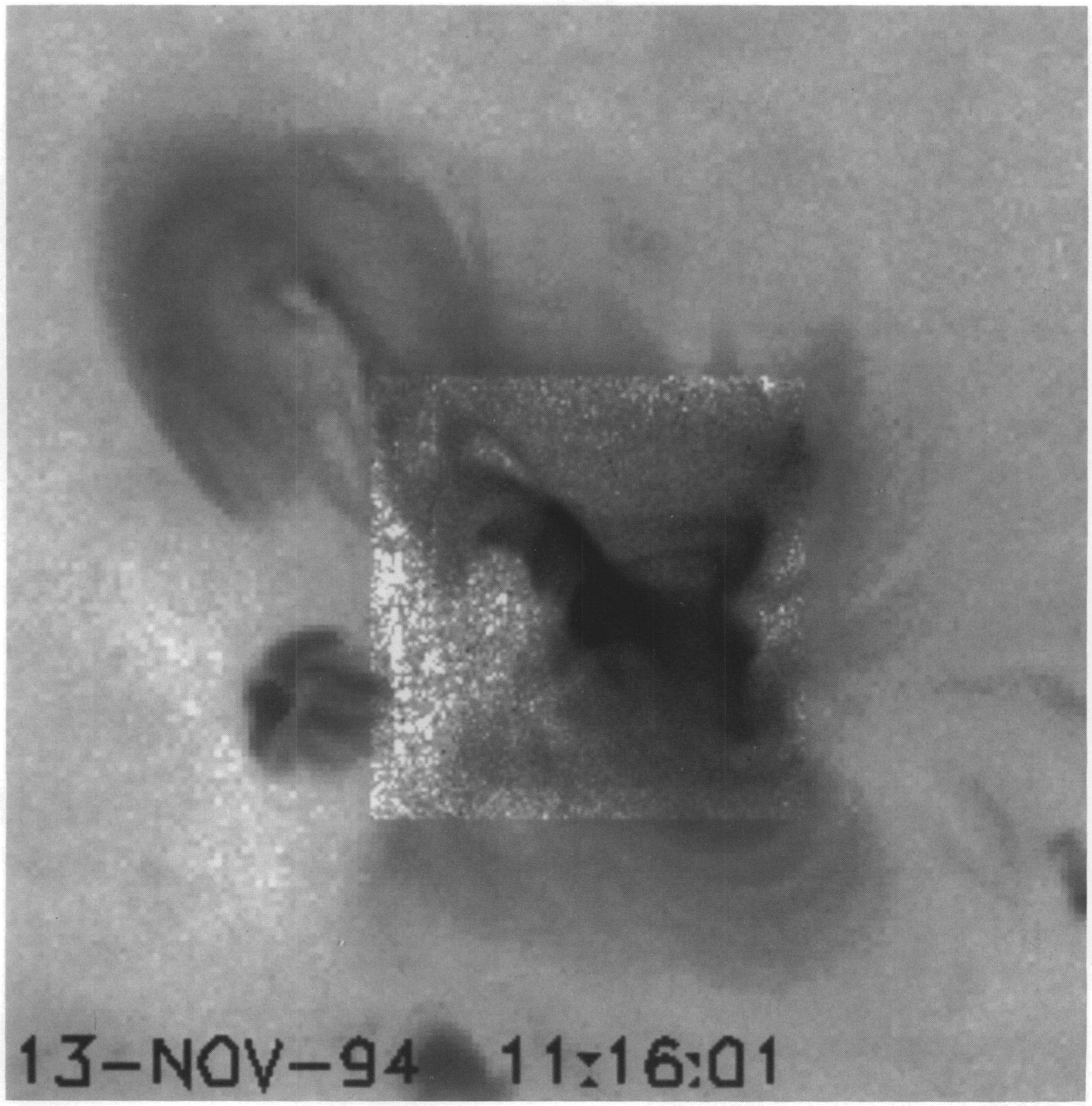

FIG. 3.—Composite image showing the high-resolution observations (2".46 $pixel^{-1}$) of the flare core overlaid on the lower resolution (4".92 pixels) observations of the nearby quiet Sun. We identify the structure to the northeast with a part of the CME hypothesized to have occurred with this event.

HUDSON, ACTON, & FREELAND (see 470, 629)

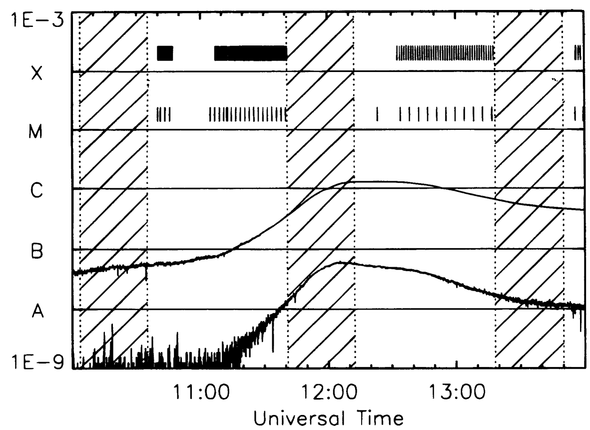

FIG. 1.—Time-series road map to the event studied here using the *GOES* soft X-ray time history. The plot indicates the times of *Yohkoh* night (*hatched*) plus the exposure times for the available full-frame (*lower ticks*) and partial frame (*upper ticks*) images. In the day period ending about 11:40 UT, *Yohkoh* observed the main flare rise in its high telemetry rate; in the orbit beginning at about 12:30 UT, the telemetry rate was medium and the resolution correspondingly lower. Flare mode did not trigger.

flare and the structure in the northeast external to it. As described in the Appendix, these motions have complicated patterns (Fig. 4 [Pl. 9]). The loops connecting the east and west branches of the core structure rise to the north with projected velocities of about 100 km s^{-1}. The motion appears to be considerably faster, and to accelerate, at the northeast and northwest cusps.

2.2. *Disappearance and Ejection of Coronal Structures*

The disappearance of the large volume to the northeast of the event core (Fig. 5) could in principle be due either to cooling below the sensitive range of SXT or to expansion. Based upon the derived parameters (see below), we can estimate a radiative cooling timescale as

$$\tau_{\rm rad} = \frac{3kT}{\Lambda n_e} \approx 1.3 \times 10^5 \text{ s} ,$$

where $\Lambda = 3 \times 10^{-23}$ ergs cm^3 s^{-1}. This is not consistent with the observed disappearance timescale ($<3 \times 10^3$ s), so on this basis we would conclude that a sudden expansion of the previously stable structure resulted in its disappearance

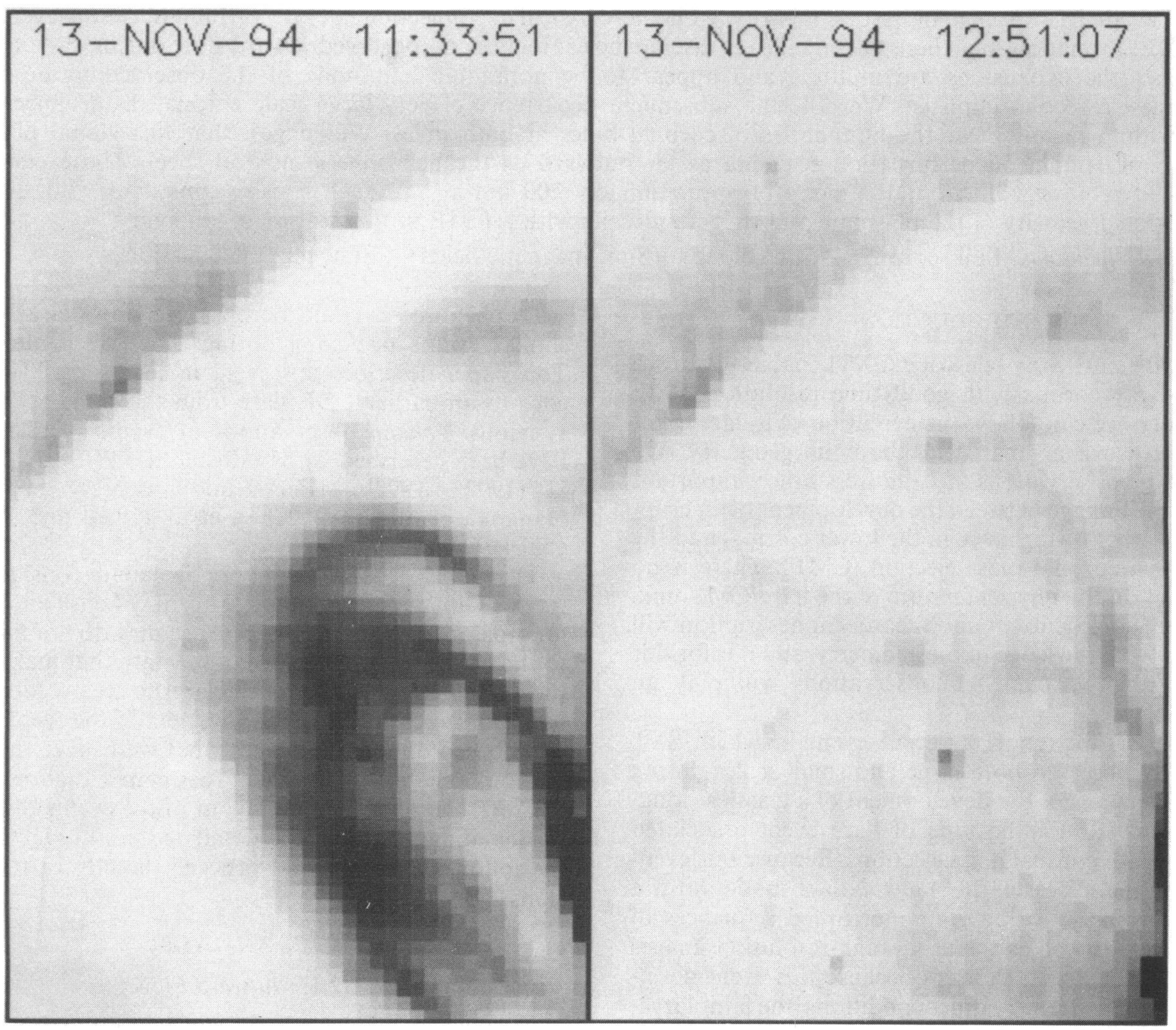

FIG. 5.—View of the coronal feature to the northeast of the flare (*left*, before; *right*, after). This feature formed well prior to the event and disappeared almost entirely from view as a result of its outward motion. Leg-like structures can be seen, especially to the west, in the "after" picture.

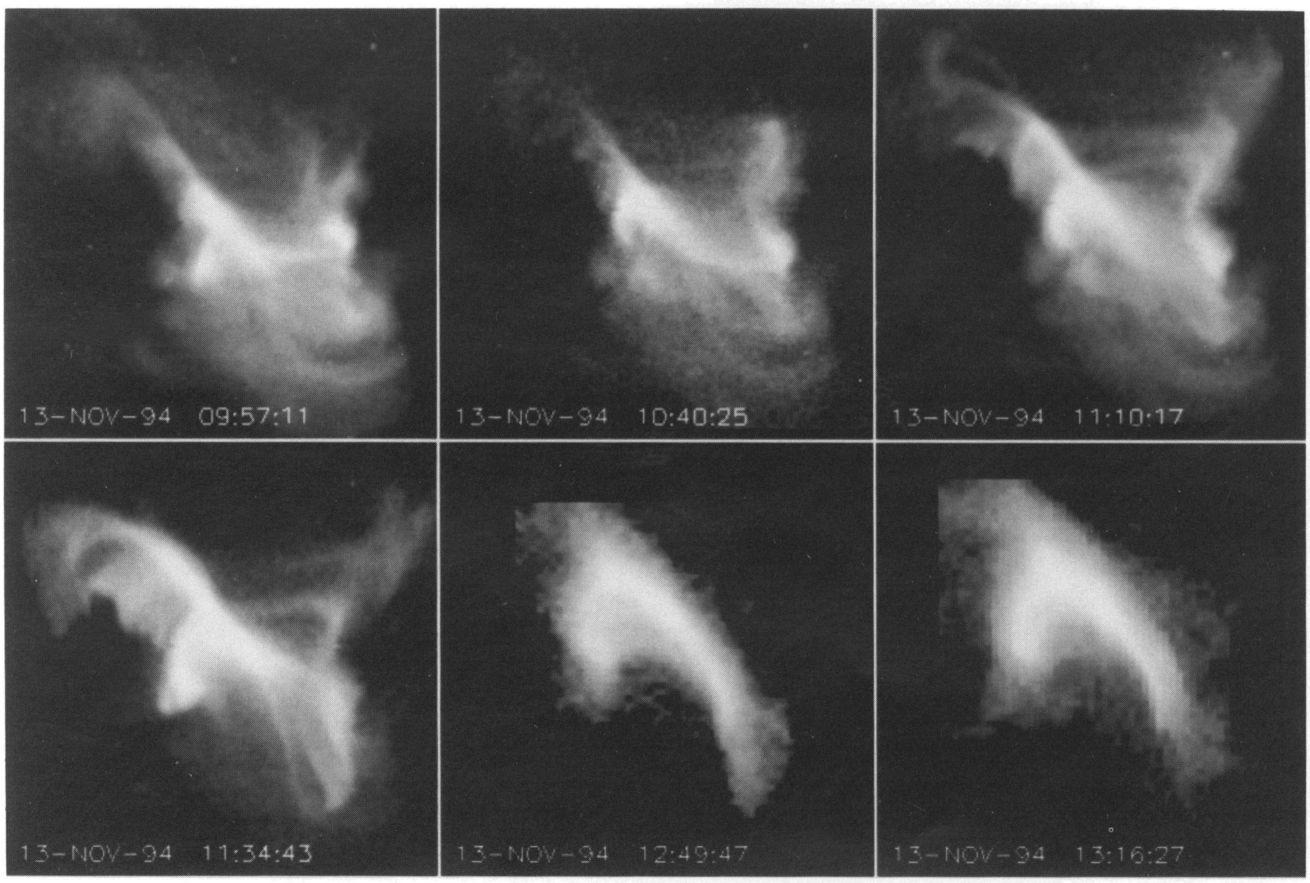

FIG. 4.—Six panels showing time development of the active-region part of the flare of 1994 November 13. These panels are each $\sim 5'$ square, with $2''.46$ pixel^{-1} in the first four and $4''.92$ pixel^{-1} in the last two. North is up and west to the right, and the images have been mutually coaligned.

HUDSON, ACTON, & FREELAND (see 470, 630)

and probable injection into the solar wind. Conductive cooling, similarly, is estimated as

$$\tau_{\rm cond} = \frac{2nkl^2}{\kappa_0 T^{2.5}} \approx 1 \times 10^4 \text{ s} ,$$

where $\kappa_0 = 1 \times 10^{-6}$ ergs (cm $K^{3.5})^{-1}$. Again, this appears to be too long to explain the disappearance, but the parameters of the conduction process (not to mention the physics itself) are less well known. Note that we have little doubt in this case that ejection actually occurred, because we can observe directly the outward motion and expansion of the cloud.

The disappearance of two regions of the diffuse corona appears to be an integral part of the overall phenomenon, and we believe that a white-light coronagraph in the right orientation would have detected a coronal mass ejection as a consequence. This confirms that at least some of the material of the coronal mass ejection, whose temperature cannot be known from the white-light intensity, can in fact originate from the high-temperature corona and need not be supplied from cooler regions of the atmosphere. This is consistent with "freezing-in" ionization temperatures measured in the solar wind during enhanced flows related to flares (Ipavich et al. 1986).

The cloud to the northeast of the flare moves outward during the rise phase of the event. We have measured this motion by recording the outermost brightening and the centroid brightening on the apparent axis of the motion, as shown in Figure 6 along with the *GOES* and SXT photometry. The projected velocity is approximately 100 km s^{-1}, probably consistent with typical flare-associated CME speeds given the extreme projection angle from this flare ($\mu = 0.95$). The motion does not give the appearance of being radially outward, since it occurs over a large range of azimuthal angles.

2.3 *Mass Estimate*

From the two filters used for the full-Sun images, we can estimate the temperature and emission measure of the disappearing material. SXT recorded two long-exposure images just prior to the disappearance (see Appendix), and we have used the standard *Yohkoh* software to subtract dark and stray light, register, and convert to temperatures and emission measures. We find the properties listed in Table 1, leading to a total mass of about 4×10^{14} g; this is a reasonable figure for a small coronal mass ejection. For this purpose, we estimated the volume as $A_{\rm HM}^{3/2}$, where $A_{\rm HM}$ denotes the area above half the maximum intensity in the Al.1 filter image taken at 11:35:59 UT. The interesting feature of these parameter estimates is the somewhat elevated temperature of 2.8×10^6 K, a value higher than the temperature of the ordinary diffuse corona. This may reflect

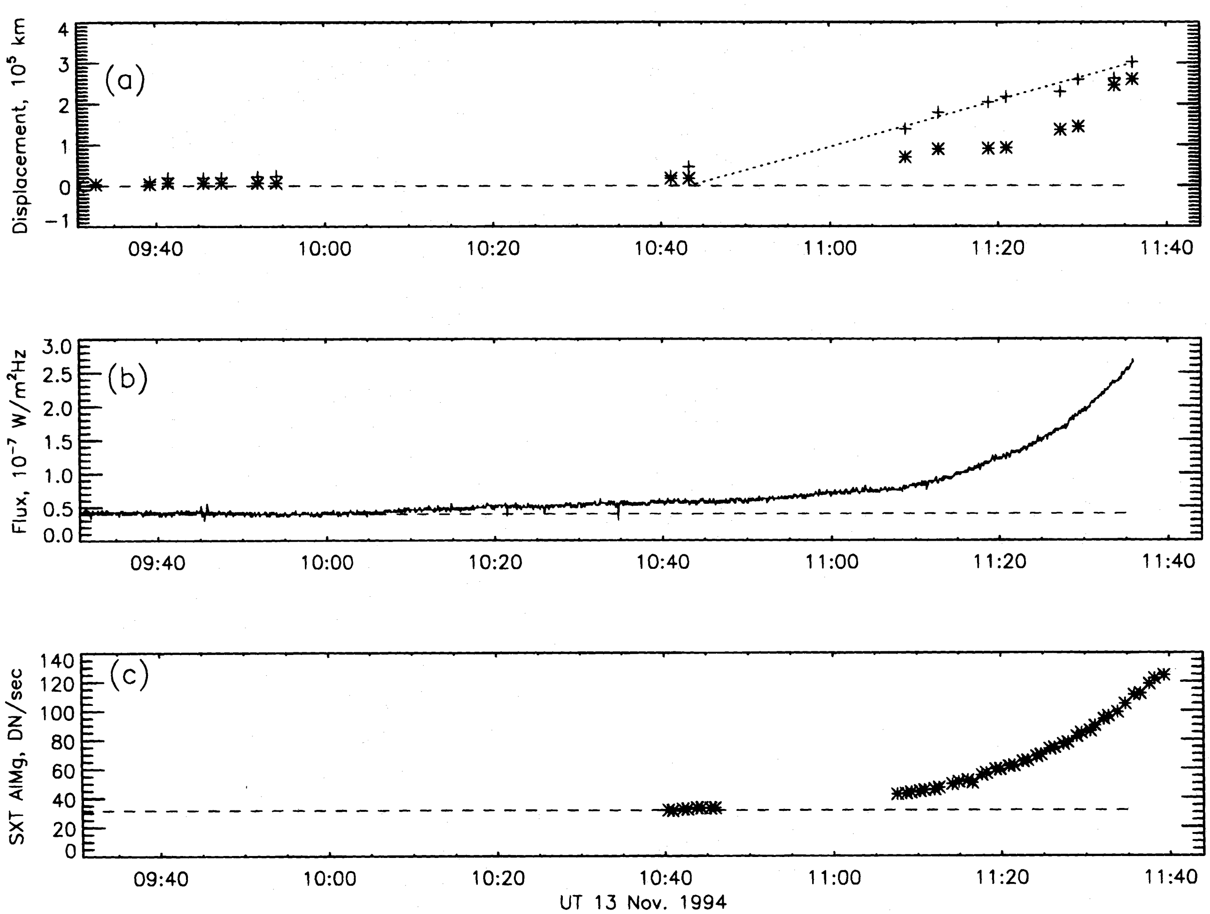

FIG. 6.—The motion of the northeast coronal cloud (*top*) showing the outermost bright feature (*plus signs*) and the brightness centroid (*asterisks*) as measured on the apparent axis of the ejection. The middle panel shows the *GOES* soft channel signal, and the lower panel shows the SXT total flare brightness. This figure shows that the onset of motion and brightening cannot be distinguished easily.

TABLE 1
PARAMETER ESTIMATES FOR EJECTED MATERIAL

Parameter	Value
Temperature (K)	2.8×10^6
Emission measure (cm^{-3})	6×10^{47}
Volume (cm^3)	9×10^{29}
Density (cm^{-3})	3×10^8
Mass (g)	4×10^{14}
Potential energy (ergs)	4×10^{29}

the fact that the large-scale structure had been created relatively recently.

We note that the mass estimate given here should be considered as a lower limit. Other coronal mass seen by SXT also disappears (e.g., to the north), but the mass estimation is difficult because of sampling and confusion problems on the line of sight. In addition, the SXT observations give more weight to higher temperature plasma, and a still larger mass of cooler material could have been ejected and/or entrained in the material SXT observed to disappear.

2.4. *Remote Consequences*: "*Aurora Solaris*"?

We would like to point out the coincidence in timing between the flare and certain remote features in the corona. These include brightenings at the north edge of the southern polar coronal hole and at the south edge of the northern polar coronal hole, the configuration of a conjugate-point auroral display on the Earth. We note also activations of interregion connecting loops between two pairs of active centers, one pair not including the flaring region itself. These large-scale events follow the flare energy release by 1–2 hr, implying an exciter speed of 100–200 km s^{-1}. This is too slow for a wave-induced excitation and triggering at the speeds normally associated with the Moreton wave (e.g., Zirin, MacKinnon, & McKenna-Lawlor 1991), and it is too slow for speeds typically associated with type II bursts. We note, however, that the inferred exciter speed resembles that of many X-ray ejecta observed by SXT (e.g., Klimchuk et al. 1994) and of CMEs (e.g., Hundhausen 1993). If the reality of such global disturbances could be confirmed in other cases, we would suggest the name "aurora solaris" by analogy with the geomagnetic substorm phenomenon. In our view, the likeliest scenario is that the flare event and inferred CME were able to destabilize larger scale structures, including the boundaries of the general heliospheric current sheet. This would explain the subsequent activity seen in both the north and south polar regions, as well as active-region interconnections.

3. CONCLUSIONS

3.1. *What Have We Seen*?

We would like to make a clear separation between this section and the next, describing here what we can see certainly, and giving our interpretations later. The phenomena occurred on three scales: the development of the core region (length scale $\sim 10^{10}$ cm), the launching of a large-scale ejection (length scale $\sim 4 \times 10^{10}$ cm), and what appear to be global aftereffects (length scale $\sim 1 \times 10^{11}$ cm).

The core region of the November 13 event evolved from a complex beginning, with copious ejecta, into a simple helmet-streamer configuration as is frequently seen in the *Yohkoh*/SXT images. The ejections occurred largely to the north, with the launching of loops mainly parallel to the magnetic inversion line. The projected velocities of the ejecta were 100–200 km s^{-1}, and the final helmet-streamer arcade was concave in the direction of Sun center. Rather than a single occurrence of ejection, this event shows repeated and almost wavelike loop expansions in much the same location, especially at the northwest. The northwest ejecta appeared to lose their structural definition as they departed from the high-resolution field of view.

On intermediate scales, we see the disappearance of large volumes of coronal material, which we associate hypothetically with an otherwise unobservable coronal mass ejection. The disappearing coronal material is to the same side of the active center as are the ejecta seen departing from the core. The disappearance of the large northeast volume discussed in the text comes after the rise phase of the flare.

On the largest spatial scales, we see disturbances in the north and south polar crown regions, and in large loop structures interconnecting active regions. We term the polar disturbances the "aurora solaris," and we believe that they were triggered by the flare. We caution that until additional cases can be documented, the possibility of a coincidental occurrence cannot be excluded entirely.

3.2. *What Do We Think We Have Learned*?

In this well-observed event, we have had an excellent opportunity to study the development of the event core at high resolution, and also the adjacent and remote corona. We find certain typical characteristics of an LDE event in these observations. Nevertheless, the standard model for events of this type, often cited in the *Yohkoh* literature as the "CSHKP" model (after Carmichael, Sturrock, Hirayama, Kopp, and Pneuman), misses in several important respects.

We see no suggestion of the inward-flowing material that is supposed to drive the magnetic reconnection. Although the inward-flowing material could exist at a temperature to which SXT is not sensitive, we note that SXT sees clearly the material north of the flare site that most likely disappeared as a result of CME formation. Instead of inflow, we see outflow, as indeed is the case of almost every event showing mass motions thus far studied in the *Yohkoh* data. The outflows that we see do not resemble the standard picture in which field lines directly above the flare location open outward in a massive destabilization; instead, they take the form of a sequence of features that we interpret as flux tubes moving sequentially away from the flare site during the rise phase. The CME launch that we infer takes place so far from the flare core that it seems quite improbable that reconnected field lines could lead back to the flare proper. The inferred CME launch also occurs well after the flare onset, in contrast to the pattern expected from the standard picture (e.g., Kahler 1992). Finally, we see nothing that could be interpreted easily as reconnection jets or slow shock fronts, either outward or inward. We note in all of this that the observations may not have been complete enough to reveal these features, or they may have been confused by the complexity of the event.

The KPNO magnetograms for this event do not show an obvious quadrupolar configuration. The event occurred in an old and simple bipolar region; a second compact bipolar structure visible to the east of the flaring region did not participate in any of the activity reported here. Thus, there is little support in this event for the alternative configuration suggested by Uchida et al. (1994) for events of this type. However, we feel that this theoretical direction needs to be pursued energetically, in view of the mismatches noted above with respect to the CSHKP picture. It may be that the Kitt Peak magnetograms we have examined do not have sufficient sensitivity to show the photospheric connections of the flaring magnetic structures properly. Finally, we note that theories not involving macroscopic reconnection may be possible: the energy would be stored remotely and developed in the flare structures via the Poynting vector as the coronal current systems evolve. The geometry involved in such theories may strongly resemble that of the classical reconnection picture (e.g., Melrose 1994).

In summary, this event presents problems for the classical scenario for LDE flares; we do not see many of the expected features, even though the basic ingredients (eruptions, postflare loops, helmet-streamer configurations) are clearly a part of the picture. Many events observed by *Yohkoh* follow the script better (e.g., Tsuneta et al. 1992a, and also the October 19 event in the same active region studied here), but in addition many show equally striking discrepancies (e.g., de la Beaujardière et al. 1995). In view of this uncertainty, we feel that it would be premature to conclude that the classical mechanisms explain flares and CME formations in general. The classical picture has such strong phenomenological support that it must be correct in some respects, but based upon the observations discussed here, we urge a much wider examination of the theoretical possibilities.

NASA supported this work under contract NAS 8-37334. The *Yohkoh* satellite is a project of the Institute of Space and Astronautical Sciences of Japan. We thank the National Solar Observatory and Big Bear Solar Observatory for archival data used here.

APPENDIX

OBSERVATIONAL MATERIAL

A1. GENERAL

The event studied here took place on 1994 November 13, in an active center at the heliographic location of NOAA active region 7790 (N15 E10) (from the previous rotation). This region had produced an LDE (*GOES* class M3) event on October 19 similar to (but about an order of magnitude more energetic than) the one discussed in this paper, which had *GOES* class C1.2. The *GOES* photometric data of the November 13 event (Fig. 1) give an appearance of simplicity, with a typical slow rise and duration of many hours, in the classical pattern of an LDE (Pallavicini, Serio, & Vaiana 1977). However, the event included a series of rapidly developing large-scale phenomena, as indicated in Figure 2 and listed in Table 2. These phenomena are too faint and too cool to show up in the nonimaging *GOES* data, which responds best to the flare core. The SXT images show abundant structure during this interval. The flare itself generally evolves toward decreasing complexity, as illustrated by the representative high-resolution images of Figure 4, accompanied by growth in scale. A movie representation provides a much more comprehensive view of the morphology. During the interval from 09:31:05 to 16:31:39 UT, SXT recorded approximately 274 high-resolution images in two filters, with an image interval of 32 s. The filter usage consisted of repetitions of the set {AlMg, Al.1, AlMg}, providing temperature determinations below about 10×10^6 K (Tsuneta et al. 1991). There were also 76 full-Sun images. Table 3 summarizes the *Yohkoh* coverage.

A2. MAGNETIC CONFIGURATION

The active center in which the November 13 events developed had, on its previous rotation (as NOAA 7790) generated another LDE flare event. Figure 7 (Plate 10) shows KPNO magnetograms from three solar rotations, illustrating the typical pattern of field diffusing and weakening in the decay of the active region.

We have coregistered the SXT images with the nearest on-line Kitt Peak magnetogram, which was taken about 31 hr after the event. Figure 8 shows overlays of this magnetogram with an SXT image of the flare, after correction for solar rotation in between the time of the magnetogram and the time of the event. This overlay is thus only approximate, but it shows that the main axis of the initial arcade and the final cusped structure follows the neutral line, and it suggests the possible existence of a magnetic structures (mixed polarities) that could explain the complicated structure seen near the beginning of the event. At the time of the flare, the field is quite diffuse and shows the network well. The well-defined footpoints of the flare loops at the time shown seem to delineate at least one network cell reasonably well.

TABLE 2

TIMELINE OF PHENOMENA

Time (UT)	Phenomenon
01:50	Twisted bilateral jet emanates from active-region core along arcade axis
10:38	Large-scale loop structure develops to NE; link expansion begins
10:38–10:47......	Ejections continue
11:07–11:41......	Ejections continue
12:38	NE structure has disappeared; link structure disappears
13:08	Completion of evolution into postflare loops
13:08	Activity at N and S polar coronal hole boundaries
13:55	Excitation of interregion loops
24:00	Eventual disappearance of postflare loops

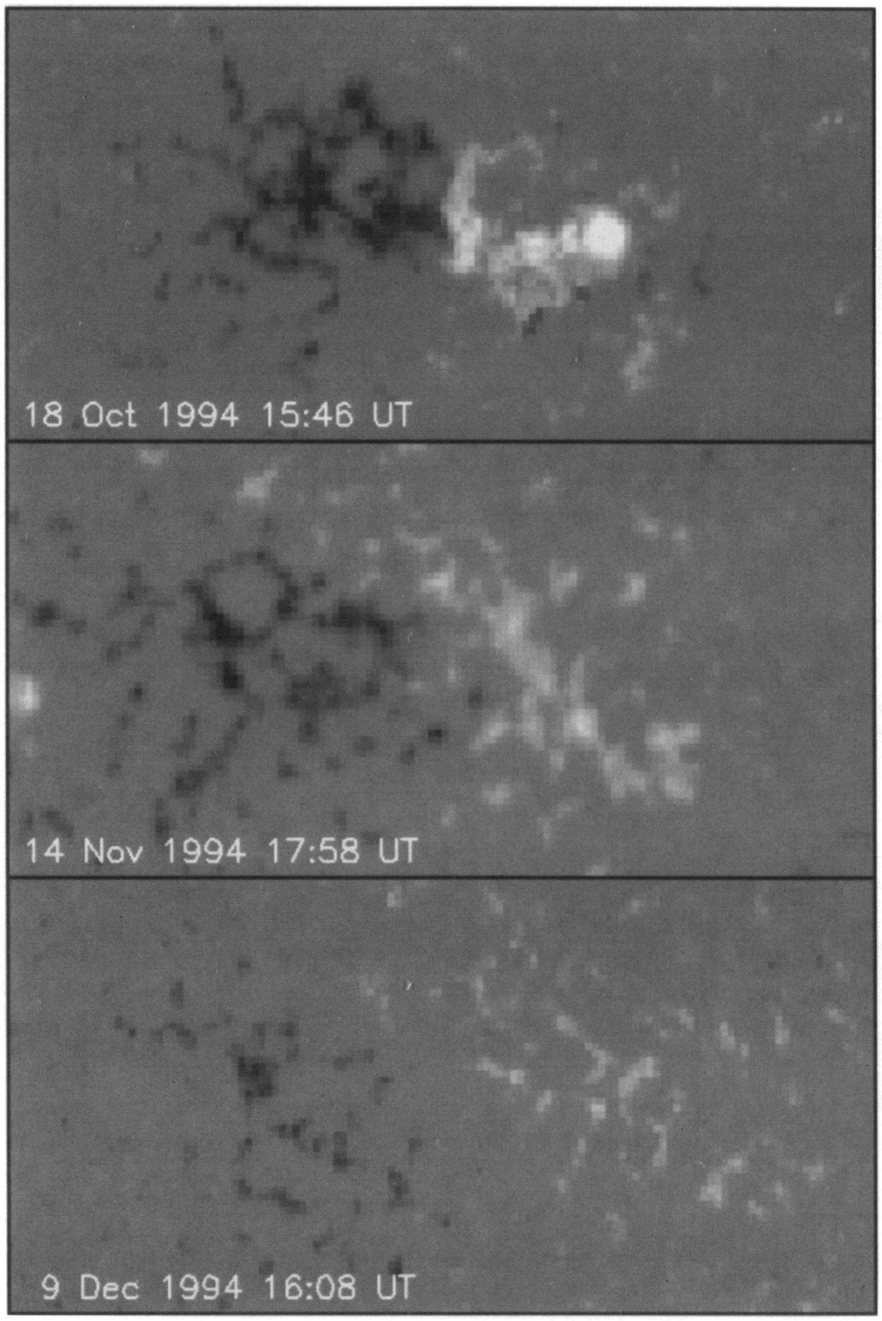

FIG. 7.—KPNO magnetograms from 1994 October 18 and November 13, at times near the event times. *Top*: The October event, when the active region showed sunspots. *Middle:* The November event described in this paper. *Bottom*: Approximately one rotation later. Note the classical pattern of diffusion and shearing of the simple bipole. At the time of the November 13 event, the region contained no sunspots.

HUDSON, ACTON, & FREELAND (see 470, 633)

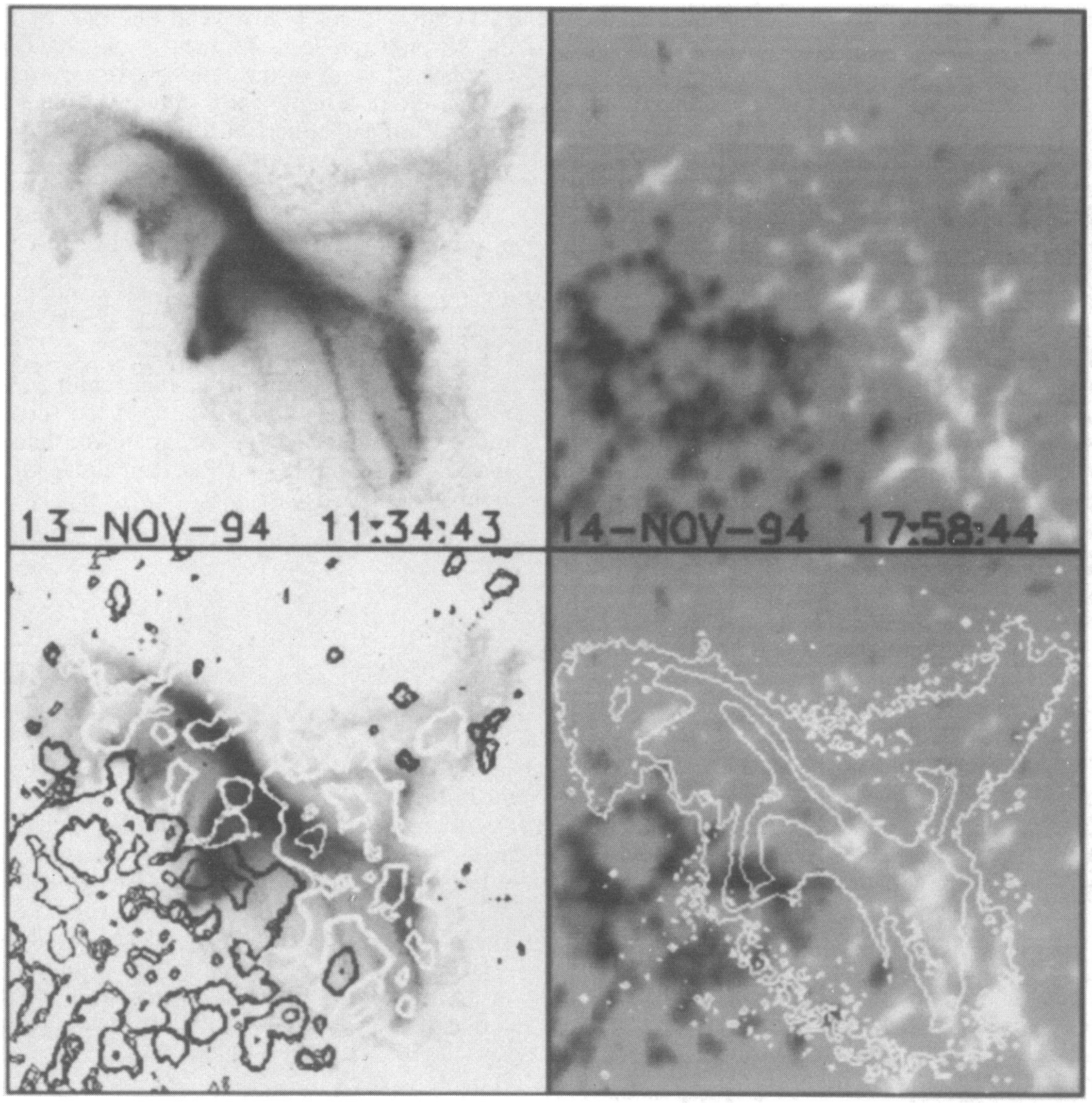

FIG. 8.—Overlays of the central core of the flare (image of 11:34:43 UT) on a Kitt Peak magnetogram taken approximately 31 hr later. *Top left*, the SXT image; *top right*, the magnetogram rotated by the differential rotation; *bottom left*, the image with magnetic contours; *bottom right*, the magnetogram with image contours. We see the general alignment of the brightest flare structure with the magnetic neutral line. The flare structure to the northwest has no obvious association, although there are mixed polarities. However, the time interval is quite long for a comparison of this type.

We do not present an analysis of the October 19 flare here. However, it was well observed by *Yohkoh* (but in the usual flare mode, so with greatly reduced whole-Sun coverage) and had features that contrast interestingly with those of the November 13 event. Specifically, we find a similar pattern of loops moving away from the bright loop arcade during the rise phase of the event. As with the November 13 event, the timing of these motions appears to match as closely as we can tell with the brightening, i.e., the rising motions extrapolate to the arcade top at the time of event onset in *GOES*. We note that such extrapolations are never very precise and that the onset time is a poorly defined quantity because it depends upon the detection threshold. In the October event, the motions are again asymmetrical, but they are to the west and south in this case. This is again inconsistent with the vertical direction for this event, which occurred at N12 W24. The projected velocity of the moving structures is also on the order of 100 km s^{-1} in this event.

A3. CENTRAL CORE

As can be seen in Figure 4, the November 13 flare brightens along a spine extending from northeast to southwest, with a separate structure to the northwest that appears to be connected to the spine via a series of looplike links. Footpoint brightening occurs during the rise phase, in a rather complicated pattern, and the arcade footpoints appear to expand to the east irregularly. Something rarely observed is happening at the same time: the interconnecting loops appear to slide continuously upward in an expanding motion. These links terminate on the west in a pointed structure, and a small open loop or cusp appears at the northeast end of the arcade. In the movie version, this process gives the appearance of shedding a sequence of layers, reminiscent of the Tesla coils seen in Frankenstein movies. The shedding process is also perceptible in the movie of full-frame images to be discussed below. Figure 3 shows that the shedding process actually accompanies a decrease

TABLE 3

SXT Observations

Time (UT)	FFI Pixel Size[a] (arcsec)	PFI Pixel Size[b] (arcsec)	PFI Field of View (arcmin)
Before 11:41......	4.92	2.46	5.24
After 12:38	9.82	4.92	5.24

[a] " Full-frame images " (whole Sun).
[b] " Partial frame images " (high resolution).

of the coronal brightness in the active-region corona to the north of the arcade. The shedding appears to be continuous, not in the form of a unique "plasmoid," filament, or blob. As the core region becomes brighter and toward the end of the rise-phase coverage at about 11:40 UT, the ejection appears to accelerate and to lose its definition in the northwest cusp region. In the final stages of development (the final two frames of Fig. 2), the links and the footpoint have disappeared, leaving postflare loops of characteristically simple shape behind.

A4. MOTIONS

The disappearing structure to the northeast of the flare core comes into existence well before the flare brightening begins, but it only starts to move at the time of the brightening (Table 2). We have not attempted a full analysis of the velocity field of this moving structure, but we have tried to track different features as they move along the apparent lines of motion. Some of the results are shown in Figure 6. It is evident that there is a close match in time between the motion itself and the flare brightening. The timing issue is an important one in discussions of the relationships between flares and CMEs, which is one reason that close-in observations of this type should be explored carefully. In this case, we see no obvious temporal delays: the motion and the onset of brightening appear to coincide.

A5. GLOBAL CORONA

In the global views of this event, we note several steps, as summarized in Table 2. The earliest major activity in the active region, a twisted bipolar jet, occurs about 9 hr before the eruption. This jet is oriented along the magnetic axis in the direction of the final cusped structure. We have no way of establishing whether or not it is related directly to the phenomena occurring later. The activity at the north and south polar hole boundaries is closer in time, and this plus the appearance of the movie indicates a physical relationship. At the north, a brightening wave runs along the polar-crown filament channel; at the south, a large-scale ejection event occurs; simultaneously, an excitation and restructuring of the loops connecting different active regions (the site of the flare to NOAA 7804; NOAA 7804 to NOAA 7805) occurs also. We note that the on-line Hα images from Big Bear Solar Observatory show the disappearance of several filaments in the vicinity of the interconnecting loops and southern eruptive event. These all provide qualitative evidence that the flare destabilized several parts of the large-scale corona, stimulating them into the activity observed.

We believe the coronal dimming seen both to the northeast and to the north, in different structures, to be causally related to the flare. Figure 3 documents this disappearance as seen within the active center, but we note that the diffuse structures seen some distance to the northeast, and continuing also to be formed during the flare proper, also disappear during the *Yohkoh* data gap between 11:35 and 12:38 UT. The SXT spectral response generally increases or is flat with temperature. If a large-scale SXT coronal structure disappears suddenly from view, it must either have cooled precipitously or expanded rapidly. As described in the text, we believe that rapid expansion is a more likely explanation, given the common association of LDE flares with coronal mass ejections (CMEs) and with the prevalence of other kinds of ejection observed here. Although no CME was observed at this time, an observation would not be expected given the location of the event near disk center.

REFERENCES

de La Beaujardière, J.-F., Canfield, R. C., Hudson, H. S., Wülser, J.-P., Acton, L., Kosugi, T., & Masuda, S. 1995, ApJ, 440, 386
Hanaoka, Y., et al. 1994, PASJ, 46, 205
Hiei, E., Hundhausen, A., & Sime, D. 1993, Geophys. Res. Lett., 20, 24
Hundhausen, A. J. 1993, J. Geophys. Res., 98, 13, 177
Ipavich, F. M., et al. 1986, J. Geophys. Res., 91, 4133
Kahler, S., 1992, ARA&A, 30, 113
Khan, J. I., Uchida, Y., McAllister, A. H., & Watanabe, Ta. 1994, in X-Ray Solar Physics from *Yohkoh*, ed. Y. Uchida, T. Watanabe, K. Shibata, & H. S. Hudson (Tokyo: Universal Academy Press), 201
Klimchuk, J. A., Acton, L. W., Harvey, K. L., Hudson, H. S., Kluge, K. L., Sime, D. G., Strong, K. T., & Watanabe, Ta. 1994, in X-Ray Solar Physics from *Yohkoh*, ed. Y. Uchida, T. Watanabe, K. Shibata, & H. S. Hudson (Tokyo: Universal Academy Press), 181
McAllister, A., et al. 1992, PASJ, 44, L205
Melrose, D. B. 1994, in Proc. Kofu Conference, NRO Report No. 360, ed. S. Enome & T. Hirayama (Tokyo: National Astronomical Observatory), 235
Pallavicini, R., Serio, S., & Vaiana, G. S. 1977, ApJ, 216, 108
Tsuneta, S., et al. 1991, Sol. Phys., 136, 37
Tsuneta, S., Hara, H., Shimizu, T., Acton, L. W., Strong, K. T., Hudson, H. S., & Ogawara, Y. 1992a, PASJ, 44, L63
Tsuneta, S., Takahashi, T., Acton, L. W., Bruner, M. E., Harvey, K. L., & Ogawara, Y. 1992b, PASJ, 44, L211
Uchida, Y., McAllister, A., Khan, J., Sakurai, T., & Jockers, K. 1994, in X-Ray Solar Physics from *Yohkoh*, ed. Y. Uchida, T. Watanabe, K. Shibata, & H. S. Hudson (Tokyo: Universal Academy Press), 161
Watanabe, Ta., Kojima, M., Kozuka, Y., Tsuneta, S., Lemen, J. R., Hudson, H., Joselyn, J. A., & Klimchuk, J. A. 1994, in X-Ray Solar Physics from *Yohkoh*, ed. Y. Uchida, T. Watanabe, K. Shibata, & H. S. Hudson (Tokyo: Universal Academy Press), 207
Zirin, H., MacKinnon, A., & McKenna-Lawlor, S. M. P. 1991, in Solar Interior and Atmosphere, ed. A. N. Cox, W. C. Livingston, & M. S. Matthews (Tucson: Univ. Arizona Press), 964